Modular Wideband High Angular Resolution 79 GHz Radar System

Conference Paper · March 2019

DOI: 10.23919/GEMIC.2019.8698121

7 authors, including:

Stefan Preussler
Technische Universität Braunschweig
115 PUBLICATIONS **806** CITATIONS

SEE PROFILE

Thomas Schneider
Technische Universität Braunschweig
270 PUBLICATIONS **2,067** CITATIONS

SEE PROFILE

Modular Wideband High Angular Resolution 79 GHz Radar System

Fabian Schwartau*, Stefan Preussler*, Markus Krueckemeier*, Florian Pfeiffer†,
Hannes Stuelzebach†, Thomas Schneider*, Joerg Schoebel*
*Institut für Hochfrequenztechnik, Technische Universität Braunschweig,
Braunschweig, 38106 Germany, Email: fabian.schwartau@ihf.tu-bs.de
†perisens GmbH, Garching, 85748 Germany, Email: pfeiffer@perisens.de

***Abstract*—This paper demonstrates a modular 79 GHz radar system based on the Texas Instruments AWR1243 radar chip. The modules are synchronized with a radio-over-fiber link to allow the combination of many modules and thus large apertures. A large aperture results in a high angular resolution, which is the key requirement for object classification at long ranges. We describe the coherent synchronization, the chosen antenna pattern, a genetic algorithm to optimize antenna weights and the overall system design. Finally, we demonstrate the capabilities of the system with measurements of a test set up.**

***Index Terms*—MIMO radar, Large aperture, Radio-over-fiber, Synchronization, Coherence, High resolution, High bandwidth, Antenna arrays, Genetic algorithm**

I. Introduction

Recent developments in the field of radar imaging and autonomous driving have created an increasing demand for sophisticated radars with a higher maximum range and improved angular or range resolution at lower cost. The high demand from the automotive industry for fully integrated radar sensors allows large volume production of highly integrated radar-on-chip (RoC) at a low price. The availability of such systems permits novel approaches to radar systems with high range and high resolution.

To achieve good radar range resolution a high bandwidth is required, which is only available at a high operation frequency. For example, the 79 GHz band provides a bandwidth of 4 GHz which allows a maximum range resolution of 4 cm [1]. Increasing the aperture and thus the number of antennas will increase the angular resolution. The challenge in setting up a radar with high angular resolution at frequencies in the 79 GHz band is to coherently synchronize multiple modules. We introduced a novel approach of synchronizing automotive radar chips using millimeter wave photonics in [2] and [3] to overcome the problems of high attenuation in long coaxial cables. The increased number of available channels also leads to the ability to measure co- and cross-polarization in a single system. This additional information can improve the classification accuracy of objects detected by the radar [4].

In the following we propose a fully coherent system based on individual modules, which utilize the Texas Instruments AWR1243 RoC. The system allows a modular arrangement of the antennas to build systems with very large apertures in the 79 GHz band.

II. Radar Chips

The Texas Instruments AWR1243 is a fully integrated 76 GHz to 81 GHz frequency modulated continuous wave (FMCW) radar chip. It features an integrated phase locked loop (PLL), three transmit and four receive channels, baseband conversion and analog-to-digital conversion. The chip has an available bandwidth of 4 GHz with a ramp slope of up to $100\,^{\mathrm{MHz}}/_{\mu\mathrm{s}}$. The maximum transmit power is 12 dBm while having a receiver noise figure of 15 dB. More detailed specifications can be found in [5] and [6].

The AWR1243 supports electrical synchronization of multiple chips, which is crucial for implementing large apertures using multiple chips. To achieve synchronization three different signals are employed:

- A common 40 MHz clock is used as main reference and drives all internal circuits. All chips will derive their local ADC and digital domain clock from it. There will be one master chip, which provides further signals for multiple slaves.
- A trigger signal generated by the master, which will synchronize the start of the analog to digital converters (ADC) for a single sweep event.
- A frequency ramp generated by the master at a quarter of the operating frequency which is about 20 GHz. The transmit signal and the LO signal used for the receiver mixers is derived from this lower frequency ramp by frequency multiplication.

The captured data from the ADCs can be read from the chip using one out of three different interfaces. The simplest interface is SPI which is also used for controlling the RoC. Due to the limited data rate of SPI more complex and fast chirp sequences cannot be performed, as the internal memory is limited. Alternatively, the radar provides an interface that can be configured as either low-voltage differential signaling (LVDS) or camera cerial interface (CSI-2) at up to 600 Mbps per lane with four data lanes available.

The chip itself comes in a 0.65 mm pitch, 161-pin flip chip ball grid array (BGA) and is fabricated in a 45 nm RFCMOS process [6]. The package has a size of 10.4 mm x 10.4 mm. The small footprint and BGA package allows a low-cost and simple production. The antennas can be placed directly on the

ISBN 978-3-9812668-9-4

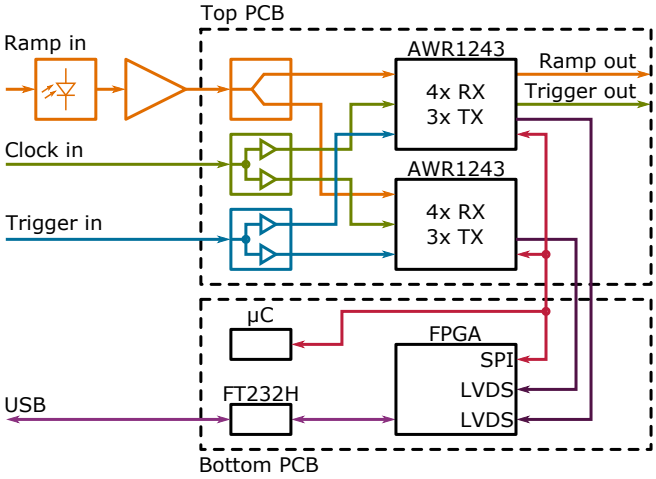

Fig. 1. Block diagram of a single module including all major components

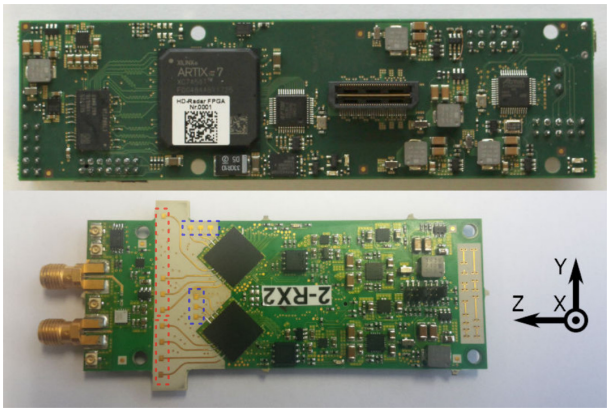

Fig. 2. Photos of the FPGA PCB (top) and the radar PCB (bottom) building a single module and the used coordinate system. The receive antennas are marked with the red boxes, the transmit antennas are marked with the blue boxes. Only the bottom three transmit antennas are used on each module.

PCB as patch antennas, which further reduces the complexity of the design.

There are many other chips with similar functionality as the AWR1243 available, which may be a suitable replacement. The key requirement is access to the ramp signal, so it can be distributed coherently. The TEF810X from NXP may be an alternative to the AWR1243, but is not further investigated. Other chips like the IWR6843/IWR1642/IWR1443/AWR1642 from Texas Instruments lack the capability of synchronizing the ramp signal.

III. Radar Modules

In order to be able to work with different antenna configurations we decided to build a system based on modules. Every module consists of two stacked PCBs. A block diagram is shown in Fig. 1 and Fig. 2 shows a photo of the PCBs of a single module. The radar PCB carries two AWR1243 radar chips, the necessary power supply and the antennas. The other board holds a microcontroller as a main control unit that configures the radar chips via a serial peripheral interface (SPI) interface and also handles the command exchange to the controlling PC. The data from the two radar chips is routed via two four lane LVDS interfaces to a field-programmable gate array (FPGA) on the bottom board. The FPGA is able to buffer the data in an onboard DDR3-SDRAM and transfers the data to the PC using USB. Each module has input and output connectors on the top board for all three synchronization signals to become either a master or a slave module depending on certain component population. The inputs for the 40 MHz reference clock and the trigger signal are both split, buffered and fed to each radar chip. The ramp signal passes a Wilkinson divider and is connected to both radar chips. A single 5 V supply is used to power the whole module.

IV. Synchronization

As mentioned above, the synchronization of the radar modules relies on three signals; the 20 GHz ramp signal, a synchronization signal and a 40 MHz reference clock signal.

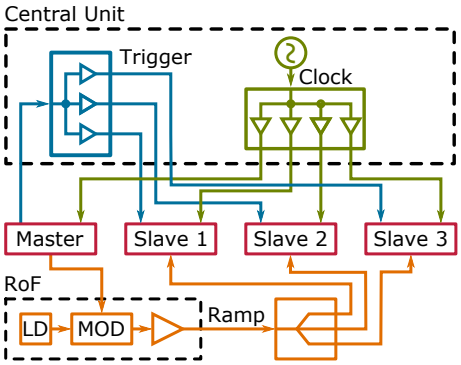

Fig. 3. Block diagram of the synchronization of multiple modules

One module is used to generate the ramp and the trigger signal, which is called the master module. These signals are generated by a single radar chip, the other one on that module is not used. The master does not participate in the actual measurement. The 40 MHz reference clock signal is generated and distributed with a clock buffering IC by a central clock management unit. This unit also splits and buffers the trigger signal, which is coming from the master module.

The ramp signal is passed to a radio-over-fiber (RoF) system described in detail in [2] and [3]. This allows long range transmission of the signal without high losses in coaxial cables and enables large aperture radar systems. The RoF system will modulate the signal onto a 1550 nm optical carrier, amplify it in the optical domain, split it into multiple fibers and bring it to each slave module. A photodiode and an amplifier mounted on each slave module are used to convert the optical signal back into an electrical signal and amplify it to the required level. The length of the optical and electrical synchronization cables does not need to be known precisely. The radar will be calibrated to compensate the signal delays. A block diagram of the synchronization of two modules is shown in Fig. 3.

ISBN 978-3-9812668-9-4

V. System Capabilities

In general, our system concept supports an arbitrary number of modules to be used as long as the signal integrity of the synchronization signals does not degrade too much. This allows a large radar systems with a huge number of individual transmit and receive antennas. All transmit and receive antennas on all modules within the system are fully coherent to each other. Together with the large aperture and high bandwidth this allows the set up of massive (pseudo) MIMO systems, which can achieve very good angular resolution, high range and reliability.

As the antennas can be arranged in any way on the PCB as long as the modules still fit next to each other, the system can be used to investigate different antenna arrangements and its effects in real scenarios. Due to this flexibility the system can be used to test and evaluate three dimensional radars, the effect of co- and cross-polarized antennas or to analyze Doppler information.

The system allows to offload signal processing from the PC to the FPGAs on each module to speed up signal processing. As an example, the 2D FFT of a chirp sequence measurement could be processed on the FPGA as shown in [7]. Admittedly, this capability of the system was not yet used for the results shown in this paper.

VI. Experimental Validation

For the experimental validation, a system with one master module and three slaves was set up. As mentioned earlier the master module does not participate in the measurement itself. Only the three slave modules will transmit and receive signals.

A. Antenna Array

The array is a linear array optimized for a low side lobe level and high angular resolution. Side lobe suppression and 3 dB-bandwidth are the key figures for the quality of an antenna array configuration. The 3 dB-bandwidth gives the theoretical resolution and thus the ability to separate two targets with equal size. The side lobe suppression limits the dynamic range in the angular spectrum and thus the ability to separate small from large targets.

We use all 8 receive channels on each module and three out of six transmit channels on each module. This gives us a total of 24 receive and 9 transmit channels. Apart from the structural restrictions, the antenna array has been optimized for a small 3 dB-bandwidth with a high side lobe suppression - especially close to the main lobe. Table. I lists the antenna positions of the used array. The resulting transmit and receive direction of arrival spectra and their combination is shown in Fig. 4.

It has to be pointed out that the radiation pattern shown in Fig. 4 is only valid for far field conditions. When estimating the far field distance using the Fraunhofer distance equation $d = {}^{2D^2}/_{\lambda}$ it results in about 32 m for an aperture D of 245 mm and a wavelength λ of 3.8 mm [8]. This does not take virtual antennas into account, which would increase the aperture even further.

TABLE I
Antenna positions in array configuration and their weights used for the measurement. The three values per cell correspond to Y/Z/W, where Y and Z are the position in mm and W is the weight.

Module 1	Module 2	Module 3
	RX	
-96.00 / 0.0 / 0.280	-38.00 / 0.0 / 0.700	96.55 / 0.0 / 0.558
-92.20 / 0.0 / 0.188	-30.40 / 0.0 / 0.854	98.85 / 0.0 / 0.204
-88.40 / 0.0 / 0.157	-22.80 / 0.0 / 0.407	105.75 / 0.0 / 0.509
-84.60 / 0.0 / 0.217	-15.20 / 0.0 / 0.665	119.55 / 0.0 / 0.223
-80.80 / 0.0 / 0.297	-7.60 / 0.0 / 0.817	133.35 / 0.0 / 0.335
-77.00 / 0.0 / 0.145	0.00 / 0.0 / 0.811	137.95 / 0.0 / 0.210
-73.20 / 0.0 / 0.250	7.60 / 0.0 / 0.913	144.85 / 0.0 / 0.417
-58.00 / 0.0 / 0.865	38.00 / 0.0 / 1.000	149.45 / 0.0 / 0.535
	TX	
-82.50 / -6.9 / 0.802	-5.50 / -6.9 / 0.697	117.50 / -6.9 / 0.454
-80.10 / -6.9 / 0.387	-3.10 / -6.9 / 0.656	119.90 / -6.9 / 0.223
-77.70 / -6.9 / 0.512	-0.70 / -6.9 / 1.000	122.30 / -6.9 / 0.084

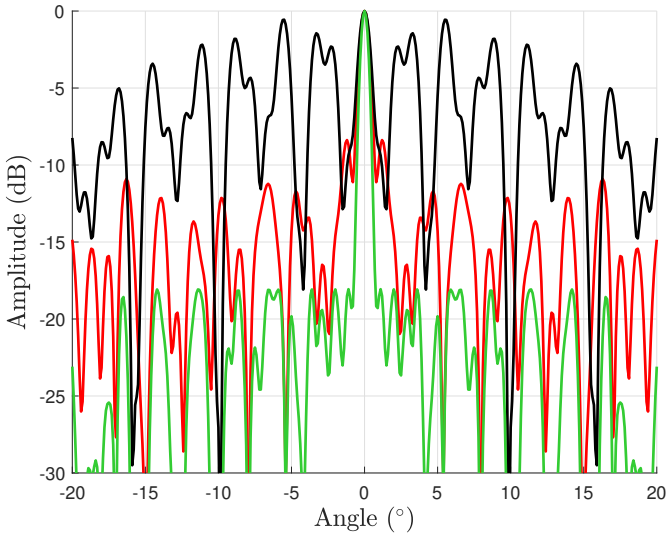

Fig. 4. Direction of arrival spectrum simulation of the receive antenna array (red), the transmit antenna array (black) and the overall transmit-receive array (green). All spectra include the weighting factors.

B. System Parameters

The Radar is configured for a short range application without moving targets. We perform a single sweep for each transmit antenna with a bandwidth of about 1.5 GHz while receiving on all 24 channels. The center frequency is 78.8 GHz, the slope of the sweep is 30 ${}^{\text{MHz}}/_{\mu\text{s}}$ which results in a maximum beat frequency of 1 MHz at a distance of 5m. Therefore the (complex) ADC sample rate is set to 5 MHz. We collect 256 samples over 51.2 μs. The target is a corner reflector with an edge length of 60 mm.

C. Signal Processing

Signal processing is performed entirely in a PC. We apply a simple narrowband phase shift delay-and-add beamforming approach [9, pp. 23–32]. The phase shift is calculated for near field conditions by defining a focus distance of the system and calculating the actual length differences between the paths and

ISBN 978-3-9812668-9-4

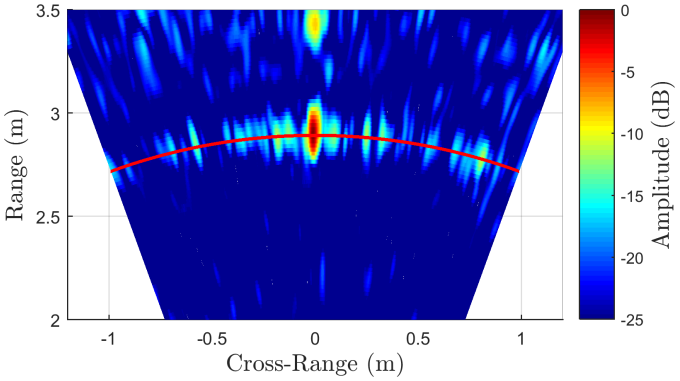

Fig. 5. Measurement of a single target in 2.9 m distance in top view. The red line indicates the cut that is shown in Fig. 6.

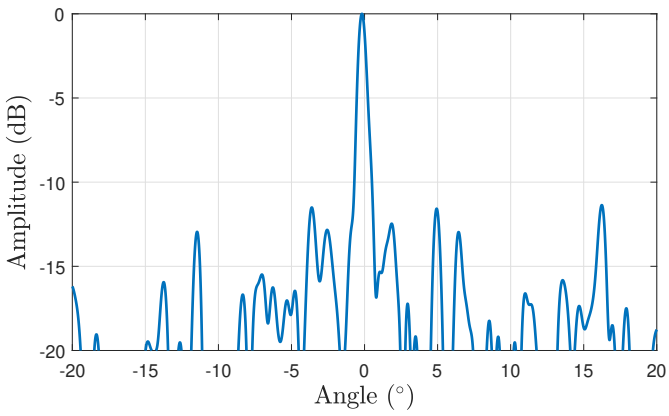

Fig. 6. Measurement of a single target in 2.9 m distance

converting them to a phase value. As the transmit and receive antenna arrays are both arranged along the horizontal axis we perform an azimuth scan.

A Hamming window is applied over the time axis to reduce side lobes in the range axis. The receive antennas are weighted to reduce side lobe levels of the radiation pattern. The weights have been calculated using a genetic algorithm, which was tuned to optimize the maximum side lobe in an azimuth range of $\pm 15\,^{\circ}$. The algorithm starts with all weights set to unity. It has a population of 10 weight sets and calculates 6000 generations. The best will always survive, the other nine children are calculated randomly. To calculate a single children two groups each with five random parents are generated. The best one in one group will reproduce with the best one from the other group by building the average value of their weights. Mutation is induced by adding random values according to $M = R_s \cdot 0.005 \cdot {R_n}^8$. R_s and R_n represent a random sign (-1, 0 or 1) and a random number in the range 0..1, respectively. This equation makes it more likely to produce smaller numbers than larger numbers, which has proven to be effective to get a fast and good convergence. When all children are calculated they are normalized such that the maximum absolute weight equals one. The weights calculated for the antennas are shown in Table. I.

D. Results

Fig. 5 shows the measurement of a single target placed 2.9 m away from the system. The target can clearly be identified at that distance and an angle of $0\,^{\circ}$. The clutter at a distance of approximately 3.4 m is caused by the stand holding the target. Fig. 6 shows a one dimensional cut of the target, indicated by the red line in Fig. 5. The measured target has a -3 dB beamwidth of $0.6\,^{\circ}$, which corresponds to the angular resolution of the system. With -11.4 dB the side lobes are higher than the simulated -18 dB in Fig. 4. This is caused by a non ideal scenario and the fact that the weights were calculated for far field conditions, which is not given.

VII. Conclusion and Future Work

We have presented a modular 79 GHz FMCW or chirp sequence radar, which allows to build large array configurations with high angular resolution. We demonstrated the system's capability to perform an azimuth scan and detect a target with an angular resolution of $0.6\,^{\circ}$. We were able to reduce the side lobes of the system employing a genetic algorithm, which optimized the weighting factors of the array. The overall synchronization of the system was achieved by employing a radio-over-fiber system.

Our future goal is to improve the system by adding more modules. This will even increase the angular resolution. The use of vertically aligned modules will allow to perform three dimensional scans and apply the system in more complex solutions. The signal processing will be improved to support three dimensional imaging. The side lobes in the angular spectrum could be further reduced by applying near field conditions to the antenna weights.

References

[1] J. Steinbaeck, C. Steger, G. Holweg, and N. Druml, "Next generation radar sensors in automotive sensor fusion systems," in *2017 Sensor Data Fusion: Trends, Solutions, Applications (SDF)*, Oct 2017, pp. 1–6.

[2] S. Preussler, F. Schwartau, J. Schoebel, and T. Schneider, "Optical signal generation and distribution for large aperture radar in autonomous driving," in *2019 12th German Microwave Conference (GeMiC)*, 2019.

[3] S. Preussler, F. Schwartau, J. Schoebel, and T. Schneider, "Photonically synchronized large aperture radar for autonomous driving," *Opt. Express*, vol. 27, no. 2, pp. 1199–1207, 2019.

[4] W. Yang, L. Jiaguo, and Z. Changyao, "A new algorithm of target classification based on maximum and minimum polarizations," in *2006 CIE International Conference on Radar*, Oct 2006, pp. 1–4.

[5] Texas Instruments, "AWR1243 Single-Chip 77- and 79-GHz FMCW Transceiver," AWR1243 datasheet, May 2017 [Revised Oct. 2018].

[6] M. Mi, M. Moallem, J. Chen, M. Li, and R. Murugan, "Package co-design of a fully integrated multimode 76-81ghz 45nm rfcmos fmcw automotive radar transceiver," in *2018 IEEE 68th Electronic Components and Technology Conference (ECTC)*, May 2018, pp. 1054–1061.

[7] H. Eugin and J. Lee, "Hardware architecture design and implementation for fmcw radar signal processing algorithm," in *Proceedings of the 2014 Conference on Design and Architectures for Signal and Image Processing*, Oct 2014, pp. 1–6.

[8] C. A. Balanis, *Antenna Theory: Analysis and Design*. New York, NY, USA: Wiley-Interscience, 2005.

[9] H. Van Trees, *Optimum Array Processing: Part IV*, ser. Detection, Estimation, and Modulation Theory. Wiley, 2004.

ISBN 978-3-9812668-9-4